LA-UR 91-2020

CONF-9107105--42

Los Alamos National Laboratory is operated by the University of California for the United States Department of Energy under contract W-7405-ENG-36.

LA-UR--91-2020

DE91 014610

TITLE: FULL-FIELD FABRY-PEROT INTERFEROMETER

AUTHOR(S): A. R. MATHEWS, R. M. BOAT, W. F. HEMSING, R. H. WARNES AND G. R. WHITTEMORE

SUBMITTED TO: 1991 American Physical Society Topical Conference
Williamsburg, VA
June 17-21, 1991

DISCLAIMER

MASTER

Los Alamos Los Alamos National Laboratory
Los Alamos, New Mexico 87545

FULL-FIELD FABRY-PEROT INTERFEROMETER

A.R. MATHEWS, R.M. BOAT, W.F. HEMSING, R.H. WARNES AND G. R. WHITTEMORE*

Los Alamos National Laboratory, Los Alamos, New Mexico 87544

This paper describes the use of a Fabry-Perot interferometer for simultaneously measuring velocity at many points on the surface of a shock-loaded solid. The method is based upon work reported by S. Gidon and G. Behar in 1986, but the data analysis has been improved by the application of image-processing techniques. Light from a pulsed single-frequency laser is focused onto a moving target and the returned Doppler-shifted image is passed through a Fabry-Perot interferometer. Output of the interferometer is a set of fringes that are formed for specific combinations of wavelength and light angle. These fringes are recorded on film for subsequent analysis. Fringe position determines the velocity for each point on the target that forms a fringe. A method for determining the velocity as a function of both position and time will also be discussed.

1. INTRODUCTION

Interferometers have become standard devices used by shockwave physicists to measure velocity history. Many variations are possible, but VISAR[1] and Fabry-Perot (FP)[2] are the most widely used optical interferometers. In both techniques, a laser illuminates a spot on the moving surface, and the frequency of the Doppler-shifted return light gives a measure of the target velocity.

In 1986, Gidon and Behar[3] described experiments in which they used a Fabry-Perot interferometer to measure velocity over an entire surface. This "Full-field" Fabry-Perot (FFP) interferometer measures the velocity at many points for a single time instead of at a single point as a function of time.

In this paper, we will present the experimental and analytical methods we are developing to make FFP a practical diagnostic tool. We will also discuss experiments that demonstrate an extension to the technique that provides a time history of the velocity over a moving surface. These techniques may prove to be useful for investigating hydrodynamic and shockwave phenomena that exhibit little or no symmetry.

2. DISCUSSION OF THE METHOD

For a typical FP experiment, a spherical lens focuses light from a single-frequency laser onto a spot on the moving target. If the spot is located near the focal point of the lens, light reflected from the target will be collected by the lens and nearly collimated as it passes into the interferometer. When the conditions for constructive interference are met, light will pass through the FP. These conditions depend upon the wavelength of the light and the FP mirror spacing. A second lens focuses the collimated light exiting the FP to form a pattern of fringes in the focal plane of the lens. As the target accelerates, the wavelength of the reflected light changes and, therefore, the conditions for constructive interference also change. As a result, the position of each fringe changes with changing target velocity, and the position of the fringes gives a measure of the target velocity.

The operation of the FFP is almost identical to the point FP. In this case, a more powerful single-frequency laser illuminates the entire target and a portion of the surrounding region. As with the point FP, light can pass through the FFP for only a discrete set of angles. If the target is stationary, light exiting the FFP will form a pattern of circular fringes whose spacing is determined by the relation[4]

$$r_{n+1}^2 - r_n^2 = \text{constant}, \qquad (1)$$

where r_n and r_{n+1} are the radii of two adjacent fringes.

As the target accelerates, the wavelength of the reflected light changes in those portions of the illuminated region that

*This work was supported by the United States Department of Energy under contract number W-7405-ENG-36.

are moving. Therefore, as the velocity changes, light from different parts of the target will satisfy the conditions for fringe formation. If the acceleration is uniform over the surface, the circular fringes in the dynamic region will move outward from their static positions. For non-uniform target acceleration, the moving fringes are not circular. The distorted pattern changes with time as different points acquire a velocity that allows reflected light to pass through the FFP. For a given fringe location, the velocity of the corresponding point on the target is given by[2,4]

$$v = k\left(\frac{R^2 - R_0^2}{R_1^2 - R_0^2} - n\right), \quad (2)$$

where k = Fringe constant in units of mm/μs
n = Fringe index
R = Position of the nth dynamic fringe (measured from pattern center)
R_0 = Radius of fringe n=0
R_1 = Radius of fringe n=1.

Velocity can then be determined by measuring the displacement of a fringe from the static position of a fringe of the same order. The velocity can be measured only at the fringe locations.

We have performed two types of experiments in the course of our FFP development. In the first, we used a pulsed (t=10 ns) Nd:YAG laser to obtain a "snapshot" of the fringe pattern produced by an electrically driven slapper. The dynamic region measured approximately 3 mm on a side. Targets of this type typically attain velocities of approximately 3 mm/μs in 1 μs. The experimental set-up is shown in Fig. 1 and the resulting fringe record is shown in Fig. 2. In the second set of experiments a dye-laser-pumped, optical amplifier, developed by Candela Laser Corporation for Los Alamos National Laboratory, boosted the power of a cw argon-ion laser (λ = 514.5 nm) from approximately 1 to 500 W for approximately 10 μs. The amplifier made it practical to use a framing camera to produce a time sequence of FFP records. The fringe record is shown in Fig. 3.

3. ANALYSIS.

Because the FFP records were in the form of photographic images, it was possible for us to perform the analysis using software originally developed for radiographic analysis. The modified software can be used for either line[5] or full-field Fabry-Perot experiments.

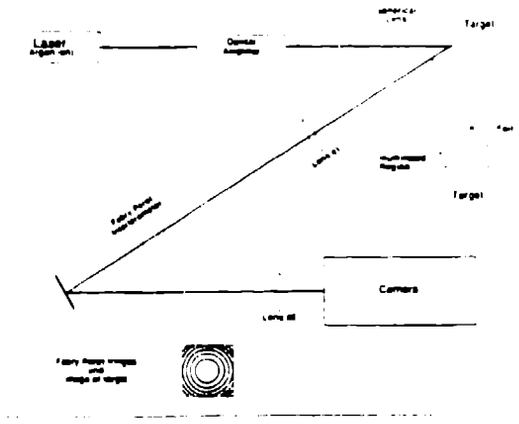

FIGURE 1
Experimental set-up. The fringe pattern formed by the second lens is either recorded directly on film (for a single frame) or directed into a framing camera (for a time sequence).

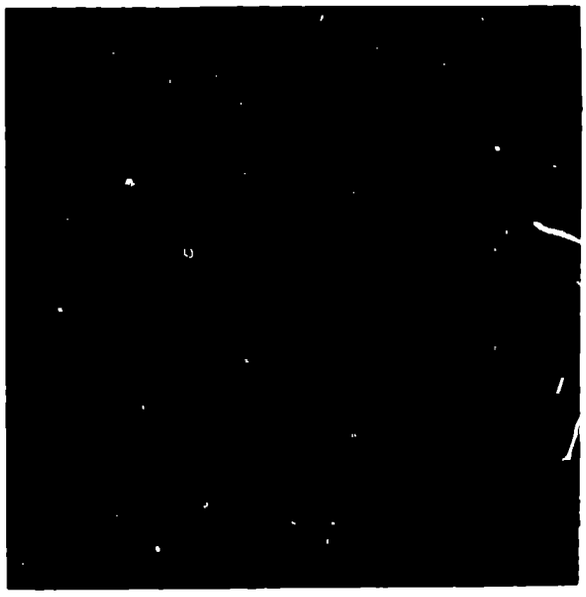

FIGURE 2
Fringe record formed by a single-pulse (t=10 ns) laser illuminating a 3-mm slapper. The illuminated region contains both static and dynamic fringes to aid correct assignment of fringe indices. The graphics overlay shows the calculated position of static fringes for a few values of n. These locations were found by solving for R in Eq. (2), with velocity set to 0.

The analysis procedure consists of determining the center of the static fringe pattern and the radii of two adjacent static fringes. For convenience, we chose two fringes outside the dynamic region and numbered them 0 and 1. Combining the measured R_0 and R_1 with the positions of the dynamic fringes, Eq. (2) can be used to determine the velocity at each fringe. The calculated velocity depends upon both the position of the dynamic fringe and the value of the fringe index, n, assigned to it. The fringe index is simply a counting scheme used to denote a change in the fringe order. Our convention is to choose n as increasing outward from the pattern center.

For our experiments, we measured the position of points of known fringe index for a few of the static fringes. A least-squares fitting procedure was then used to solve for the pattern center and radii of the first two fringes. The positions of the remaining static fringes were then determined by solutions of the velocity equation for $v = 0$. A graphic overlay of the static fringes made it relatively straightforward to follow a given fringe as it passed from the static to the dynamic region. In this manner, we hand-traced each fringe in the dynamic portion of the record. After transforming these measurements to a coordinate system whose origin lay at the center of the static pattern, we used Eq. (2) to find the velocity at every point on the fringe. The velocity distribution for the single-frame experiment is shown in Fig. 4.

FIGURE 3
Changing fringe patterns demonstrate motion in this time sequence of FFP snapshots recorded by a framing camera. Successive frames alternate from bottom to top with time increasing to the right. The time interval between successive frames is approximately 50 ns. The target in this example is a thin foil glued to a 1-mm slapper.

To aid visualization of the continuous velocity distribution over the surface, we used a linear interpolation scheme to estimate the velocity between fringes. Figure 5 shows the velocity surface obtained by interpolating the data shown in Fig. 4.

In the second set of experiments, we attempted to measure the time evolution of velocity over the surface of a fast-moving target. A framing camera recorded the time sequence as a series of individual FFP frames. After registering each fringe pattern to a common center, we measured velocities for each frame using the single-frame procedure discussed earlier. The graphic overlay of static fringes was used to check the accuracy of the registration and to aid in assigning fringe index values to the dynamic fringes. This is especially important for new fringes that formed in fast-moving areas.

As with the previous example, we hand-traced the dynamic portion of each frame and used Eq. (2) to determine the velocity

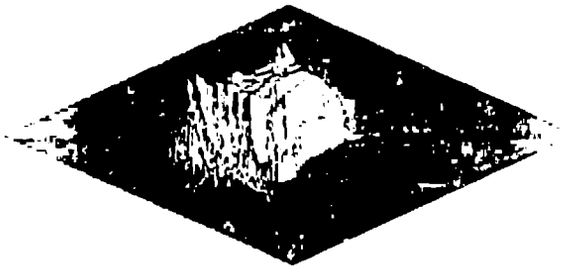

FIGURE 4
Velocity measured along each fringe.

FIGURE 5
Fig. 5. Simplex interpolated velocity distribution for the single- frame FFP experiment. The velocity surface has been rotated 90 degrees ccw with respect to Fig. 4.

along the fringes. The interpolated velocity distribution was calculated for each frame. Two frames from the resulting time sequence are shown in Fig. 6.

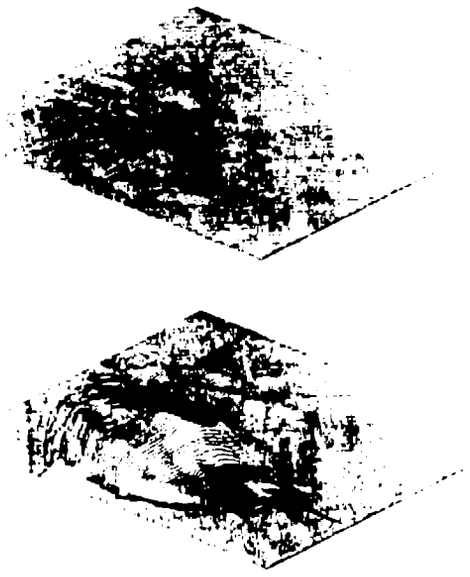

FIGURE 6
Time evolution of velocity for a moving surface. The time interval between the two frames is approximately 200 ns.

4. CONCLUSIONS.

We have demonstrated that a Fabry-Perot interferometer can be used to provide a simultaneous measure of velocity at many points on a moving target surface. The same technique was used to measure velocity as a function of time for many points on the surface. The FFP measured velocity only at discrete locations, so interpolation was used to obtain a continuous velocity distribution. This procedure does not add any new information, but provides a means by which the experimenter can more easily visualize the shape of the velocity distribution.

We are confident that the single-frame FFP provides a good quantitative velocity measure, but we cannot presently make such a claim for the time sequence. In the single-frame experiment, the fringe pattern was recorded directly on film, so little or no distortion occurred. For the time sequence, however, the framing camera introduced distortions that were not included in the analysis. We are presently working on methods to correct the camera distortion and increase the image resolution.

In the future, we will improve our method for determining dynamic fringe position. For example, the FFP analysis software can be modified to fit the line profile for each fringe. We are currently using this technique in our point FP analysis and have demonstrated sub-pixel accuracy ($\sim 25\ \mu$m) in fringe measurements. In addition, we are constructing an optical-fiber array to convert a square image to a line. This method would allow us to continuously record an FFP image on a streaking camera. Each line from the streaked image could then be converted back to a rectangular array and analyzed in a manner similar to the framing camera record.

As the quantitative accuracy of the technique improves, we intend to incorporate it into our standard assortment of hydrodiagnostics.

REFERENCES

1. L. M. Barker and R. E. Hollenbach, *J. Appl. Phys.* **43** (1972) 4669.

2. M. Durand, P. Laharrague, et al., *Rev. Sci. Instrum.* 48 (1977) 275.

3. S. Gidon and G. Behar, *Appl. Opt.* **25** (1986) 1429.

4. C.F. McMillan, D.R. Goosman, et al., *Rev. Sci. Instrum.* 59 (1988) 1.

5. A.R. Mathews, R.H. Warnes, et al., *Proc. SPIE* **1346** (1990) 122.